Available online at www.sciencedirect.com
SCIENCE DIRECT®
Journal of Crystal Growth 269 (2004) 377–384
JOURNAL OF CRYSTAL GROWTH
www.elsevier.com/locate/jcrysgro

Low-temperature liquid-phase epitaxy and optical waveguiding of rare-earth-ion-doped $KY(WO_4)_2$ thin layers

Y.E. Romanyuk[a,*], I. Utke[a], D. Ehrentraut[a,1], V. Apostolopoulos[a], M. Pollnau[a], S. García-Revilla[b], R. Valiente[b]

[a] *Advanced Photonics Laboratory, Institute of Imaging and Applied Optics, Swiss Federal Institute of Technology, CH-1015 Lausanne, Switzerland*

[b] *Departamento Física Aplicada, Facultad de Ciencias, Universidad de Cantabria, Avda. de Los Castros s/n, E-39005 Santander, Spain*

Received 1 May 2004; accepted 6 May 2004

Available online 20 June 2004

Communicated by Dr M. Schieber

Abstract

Crystalline $KY(WO_4)_2$ thin layers doped with different rare-earth ions were grown on *b*-oriented, undoped $KY(WO_4)_2$ substrates by liquid-phase epitaxy employing a low-temperature flux. The ternary chloride mixture of NaCl, KCl, and CsCl with a melting point of 480°C was used as a solvent. X-ray diffraction, differential-interference contrast microscopy, and profilometry confirmed that the layers were oriented in [0 1 0] direction with a thickness of 5–10 μm. Tb^{3+}, Dy^{3+}, or Yb^{3+} ions were incorporated into the $KY(WO_4)_2$ host, and their distribution coefficients were estimated by electron-probe microanalysis. The layers were crack-free and solvent inclusions could not be found, although the presence of secondary phases in the solution has been observed. The high optical quality of the layers was confirmed by the demonstration of passive and active planar waveguiding.

PACS: 81.15.Lm; 68.55.−a; 42.70.Hj

Keywords: A3. Liquid-phase epitaxy; B1. Rare-earth compounds; B1. Tungstates

1. Introduction

$KY(WO_4)_2$ (hereafter abbreviated as KYW) crystals belong to the family of monoclinic double tungstates, which are well known as hosts for lamp- and diode-pumped solid-state lasers and as Raman self converters [1–3]. The optically active rare-earth (RE) ions can easily substitute the Y^{3+} ion and doping levels up to 100% are possible [4].

*Corresponding author. Fax: +41-21-6933701.
E-mail address: yaroslav.romanyuk@epfl.ch (Y.E. Romanyuk).
[1] Present address: Institute of Multidisciplinary Research for Advanced Materials, Tohoku University, 2-1-1 Katahira, Aoba-ku, 980-8577 Sendai, Japan.

0022-0248/$ - see front matter © 2004 Elsevier B.V. All rights reserved.
doi:10.1016/j.jcrysgro.2004.05.049

Laser emission from a number of RE ions in KYW has already been demonstrated in pulsed and continuous-wave mode [5]. Because of the low laser thresholds, high efficiencies, and third-order nonlinear effects present in RE-ion doped KYW, it is a promising laser material both for bulk and thin-layer geometries.

Bulk KYW crystals have been grown by the top-seeded solution growth (TSSG) and the induced nucleated floating crystal (INFC) method [6,7]. Because of a polymorphic phase transition at 1015°C, crystals of the low-temperature α−KYW modification cannot be grown from the stoichiometric melt but must be grown from solution. K_2WO_4 and $K_2W_2O_7$ in different concentrations have been employed as suitable solvents [6–8]. These tungstate fluxes do not contain any ions other than those required for the crystal growth, and growth rates of 0.2 mm per hour in *b*-direction are possible. The $K_2W_2O_7$ solvent allows lower growth temperatures and apparently offers better crystalline quality [9]. Suitable degrees of supersaturation in the temperature range of 875–950°C can be achieved and bulk KYW boules with a length of up to 80 mm can be grown by TSSG.

Thin film growth of a double tungstate was reported by Atanasov et al. [10]. Pulsed laser deposition (PLD) after ablation of a stoichiometric single-crystal target was used to obtain thin films of Nd-doped $KGd(WO_4)_2$ (KGdW), which is a compound related to KYW. The films were polycrystalline and optically active, with a thickness of about 0.7 μm. However, problems related with deviation from stoichiometry, formation of unwanted phases such as $Gd_2(WO_4)_3$ or a high-temperature β-KGdW modification, and amorphization of the films appeared.

Besides PLD, which is an off-equilibrium process, liquid-phase epitaxy (LPE) is another suitable method for thin-layer fabrication of various optical materials [11]. Because of the possibility to control a low supersaturation and growth rate, LPE operates under near-equilibrium conditions and allows to produce high-quality single crystalline layers. In this paper, we report on the LPE growth of RE-ion-doped KYW thin layers onto undoped KYW substrates. The ternary NaCl–KCl–CsCl eutectic mixture [12] was employed as a solvent. This solvent was previously applied to the growth of $BaSO_4:Mn^{6+}$ [13–16]. This chloride mixture with a melting point of 480°C allows growth temperatures as low as 540°C, which is about 300°C lower than typical growth temperatures from the tungstate solutions mentioned above. Low growth temperatures can favorably reduce the thermal stress due to the differences in thermal expansion coefficients of substrate and layer at moderate to high dopant concentrations.

2. Layer growth

2.1. Solubility of KYW in the ternary NaCl–KCl–CsCl solvent

In order to establish optimum growth conditions, we investigated the solubility and stability of KYW in the chloride solvent by the dissolution–extraction method. Chlorides with purities better than 99.997 wt% were dried at 200°C for 20 h and the eutectic composition of 30.4, 24.4, and 45.2 mol% of NaCl, KCl, and CsCl, respectively, was thoroughly mixed to be used as a solvent. Fifty grams of the mixture were filled into an alumina crucible and placed without lid in a resistance-heated furnace. The solvent was heated above the melting point and then kept at a constant temperature of 550°C. Small KYW pieces of 1–5 mm in size were cut from a single-crystal KYW boule, placed onto an alumina holder, and immersed into the solvent. The chloride solvent has a rather low viscosity at 550°C, which is comparable to the viscosity of $1.6 \times 10^{-3}\,g\,cm^{-1}\,s^{-1}$ of the KCl–CsCl eutectic at 650°C [17]. The holder was rotated at slow speed for better homogenization of the solution. The temperature field inside the solution was homogeneous within 1 K. The crystals were removed from the solvent after every 12 h, weighed, and then immersed back.

The temporal evolution of the dissolved crystal mass is shown in Fig. 1 together with the calculated average dissolution rate. The total dissolved mass increases gradually with time and the dissolution rate decreases. However, the

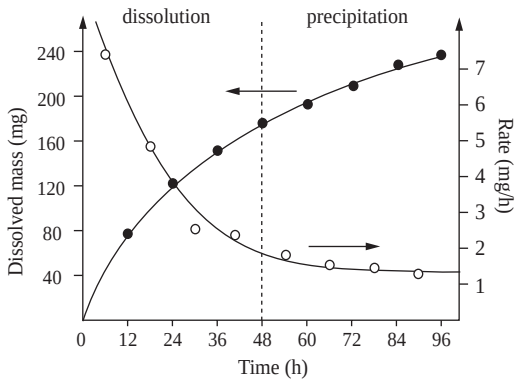

Fig. 1. Dissolution of KYW crystals in the NaCl–KCl–CsCl solvent at 550°C.

dissolution rate did not decrease to zero even after 96 h, i.e., dissolution continued. This behavior was provoked by the deposition of dissolved material on the crucible bottom. After quenching the solution, we found a polycrystalline deposit on the bottom, which was identified using powder X-ray diffraction (XRD) as a mixture of yttrium–tungsten oxides, $nY_2O_3 \times mWO_3$, with Y_2WO_6 and $Y_6W_2O_{15}$ as predominant phases. Thus, there is a dynamic equilibrium in the solution, which can be expressed by the following scheme:

$$KY(WO_4)_{2(solution)} \rightarrow nY_2O_3 \times mWO_3\downarrow_{(deposit)} + K^+_{(solution)} + (WO_4)^{2-}_{(solution).}$$

The continuous precipitation of yttrium- and tungsten-containing oxides on the bottom of the crucible shifts the equilibrium to the right-hand side in the above scheme, and the conventional determination of KYW solubility versus temperature is, therefore, impossible. The curve of the dissolution rate versus time presented in Fig. 1 can be described by two components. During the initial part (approximately 48 h), an exponential decay of the dissolution rate is dominant, because the solution gradually saturates with KYW. After approximately 48 h, the dissolution rate tends to stabilize at a rate >1 mg/h, because the continuing formation and precipitation of secondary phases removes ions from the saturated solution and, thus, triggers the dissolution of new portions of KYW. Under the assumption that the solution was saturated with respect to KYW after approximately 48 h, the solubility is about 0.34 wt% at 550°C. The change of solution mass due to the volatility of solvent chlorides was only about 0.4% and could be neglected.

2.2. Epitaxy from a solid–liquid coexisting solution

Since the precipitation of yttrium- and tungsten-containing oxides on the crucible bottom continuously decreases the amount of KYW dissolved in the solution, a sufficient concentration of KYW has to be enforced during the whole epitaxial growth. This was achieved by LPE from a solid–liquid coexisting solution. This technique implies the layer growth onto a substrate in the presence of a solid deposit of the grown phase, as was described for the first time by Kawaguchi et al. [18]. These authors demonstrated the successful growth of high-quality $LiNbO_3$ layers on $LiNbO_3$ substrates in the presence of a $LiNbO_3$ solid phase on crucible walls and proved that a low supersaturation could be achieved.

The solid KYW phase on the crucible bottom was formed by adding an excess of solute in the growth system. KYW was introduced as a stoichiometric mixture of YCl_3, K_2CO_3, and WO_3 powders with purity better than 99.99%, which form KYW in the liquid solution according to the chemical reaction

$$YCl_3 + 2K_2CO_3 + 2WO_3 \rightarrow KY(WO_4)_2 + 3KCl + 2CO_2\uparrow.$$

The initial amount of solute components was equivalent to 1–5 wt% of KYW with respect to the solution mass. Doping ions Tb^{3+}, Dy^{3+}, or Yb^{3+} were introduced as respective chlorides. The solution components were thoroughly mixed in nitrogen atmosphere with the dried eutectic mixture of chlorides and heated in an alumina crucible under ambient atmosphere at a rate of $90\,K\,h^{-1}$ to 550°C. At this temperature, the solution was homogenized for 6 h. Naturally, not the whole amount of KYW could be dissolved in the solvent at 550°C, and an undissolved crystalline deposit was present on the crucible bottom. The deposit contained KYW as a primary phase with an admixture of the above described

yttrium–tungsten oxides. Therefore, the solution was always saturated with respect to KYW because of continuous feeding of the solution with KYW due to the presence of solid KYW deposit on the bottom.

The *b*-oriented KYW substrates of $10 \times 5 \times 2\,mm^3$ in size were cut from a bulk crystal grown by TSSG and both sides were polished to laser grade quality. The substrate was mounted in a vertical position with Pt-wires on an alumina rod and placed above the crucible. After homogenizing the solution, a continuous cooling rate of $0.67\,K\,h^{-1}$ was applied and the KYW substrate was immediately immersed into the liquid. The LPE growth lasted for 24–30 h and the substrate was rotated at 15–20 rpm. By applying a cooling ramp, a supersaturation was achieved and KYW layers could be grown from the solid–liquid coexisting solution. The presence of other secondary phases certainly complicates the equilibrium in the solution. Nevertheless, the growth of pure KYW layers is possible, because homoepitaxy of KYW layers on KYW substrates is energetically favored due to perfect lattice fit.

After the growth, the layers were slowly withdrawn from the solution but kept inside the furnace and cooled down to room temperature within 24 h. Since the chloride solvent is highly soluble in water, flux droplets were easily removed from the layer surface by rinsing with distilled water.

3. Layer characterization

3.1. Growth mode

Typically, the growth started with the nucleation of three-dimensional (3D) islands on the substrate. An example is shown in the differential-interference contrast (DIC) photograph in Fig. 2(a). The islands possessed a habit of rectangular platelets, which were oriented along the crystallographic directions. α-KYW crystallizes in the monoclinic space group C2/c (recommended by the International Crystallographic Union [19]), or I2/c (normally used for orientation of bulk crystals [5]). In Figs. 2–3, we used the I2/c notation with a

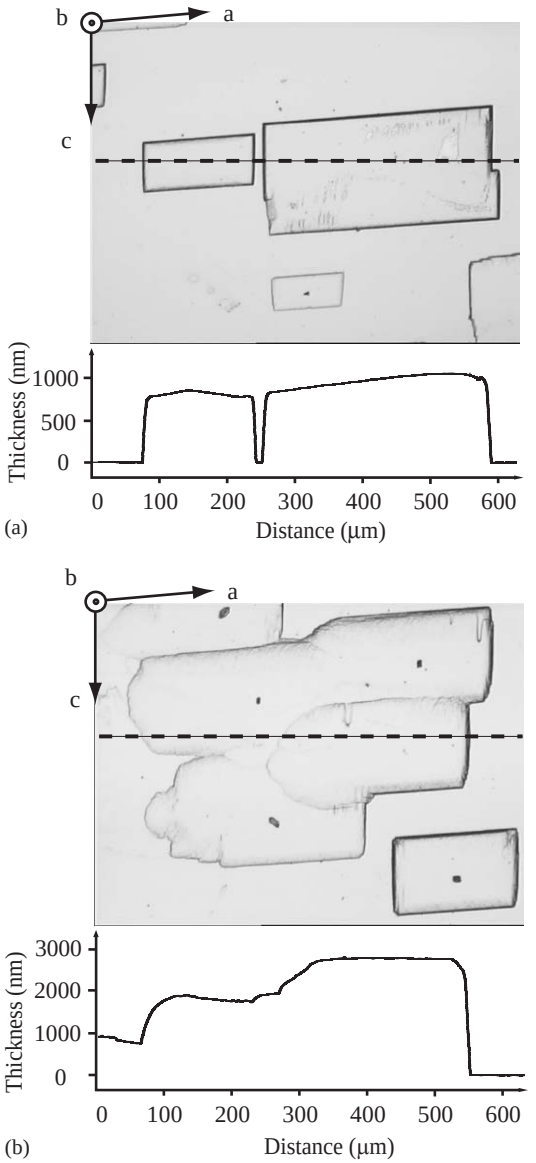

Fig. 2. DIC photographs and profiles illustrating the initial stages of layer growth: (a) growth of individual 3D islands for KYW:10%Yb; (b) coalescence of the islands for KYW:2%Dy.

monoclinic angle of 94°, because it correlates better with the morphologic habit of KYW crystals and layers (Table 1). The observed 3D nucleation is also known as the Volmer–Weber growth mode [21]. This mechanism occurs typically when the interfacial energy between layer and substrate is considerable, i.e. for large lattice

misfit, and when substrate surface energy is lower than layer surface energy. Both arguments do not apply to our epitaxy, because the RE-ion concentration did not exceed 10 at% with respect to Y^{3+} (misfit $\leqslant 0.1\%$), and we considered the growth as almost homoepitaxial. This phenomenon may hence be attributed to the low concentration of nucleation centers on the surface of the substrate, which limits the number of developing islands. Once these islands have coalesced, nucleation steps are generated and the islands start to grow arbitrarily in shape, see Fig. 2(b).

After island coalescence, the layer continues to grow with a tendency to facet formation, as can be recognized in Fig. 3. Well-developed pyramids alternated with macro-steps, which were distributed over the whole area of the layer as a consequence of the step-bunching growth process. From the average values of inter-step distance and step height, we derived a misorientation angle of $\alpha = 0.18^{\circ}$ (see Fig. 3), which corresponds to the precision of substrate orientation.

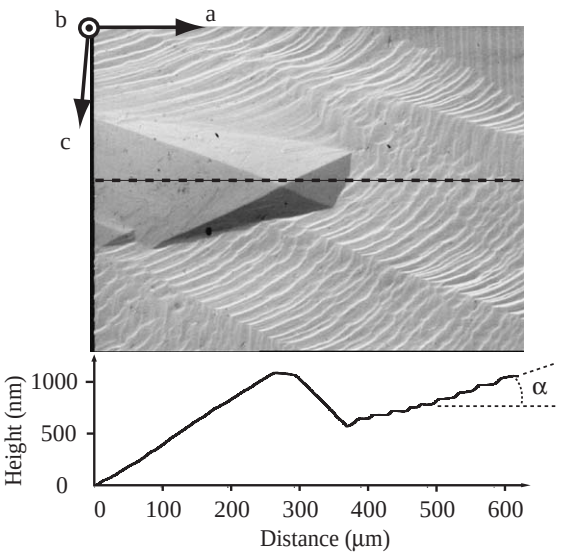

Fig. 3. DIC photograph and surface profile of an undoped KYW layer with 15-μm thickness. A faceted pyramid coexists with macro-steps, which are distributed over the whole area of the layer.

The layer thickness was typically 5–10 μm after 24 h of growth, which gives a mean growth rate in *b*-direction of approximately 0.3 μm/h, or 5 unit cells/min. At dopant concentrations above 2 at% of Yb^{3+} ions or 5 at% of Tb^{3+} or Dy^{3+} ions, the formation of a crack network was often observed, especially on the edges of the substrate. The layer was thicker and less uniform at the edges of the substrate because of higher solute feeding of edge regions due to vertical rotation of the substrate. The thickness was maximum for Yb^{3+}-doped layers, although the probability of crack formation was also highest because of the highest lattice misfit (Table 1).

3.2. Orientation and crystallinity

The layers were checked for phase purity by XRD using an X'Pert Philips diffractometer in Bragg–Brentano geometry with CuK_{α} radiation. Only (0 2*n* 0) reflections of the low-temperature α−KYW phase could be observed on all diffraction patterns of the layers grown on *b*-oriented KYW substrates. Together with microscopic observations, it shows that the layers were strictly oriented in the [0 1 0] direction and no other grain orientations were found. However, since the lattice mismatch between KYW:RE and KYW is rather low even for 100% doping (Table 1), the substrate peaks shielded the layer peaks. Only at elevated dopant concentrations or high 2θ angles the layer

Table 1
Lattice parameters of KREW crystals in the space group I2/c and lattice misfit with KYW at room temperature [20]

Compound	*a* (Å)/misfit with KYW (%)	*b* (Å)/misfit with KYW (%)	*c* (Å)/misfit with KYW (%)	*β* (°)
KYW	8.05/—	10.35/—	7.54/—	94
KTbW	8.07/0.25	10.38/0.29	7.54/0.00	94
KDyW	8.05/0.00	10.32/−0.29	7.52/−0.27	94
KYbW	8.01/−0.50	10.24/−1.06	7.47/−0.93	94

peak could be discriminated. Fig. 4 represents the (0 10 0) Bragg reflection of a 5-μm thick Tb-doped KYW layer on a *b*-oriented KYW substrate. Reflections of the $CuK_{\alpha 1}$ and $CuK_{\alpha 2}$ wavelengths from the (0 10 0) plane of layer and substrate gave rise to four peaks, which were fitted with four Lorentzian functions. From the difference in positions of the layer and substrate peaks we could estimate the content of Tb^{3+} in the layer to be 13 at% with respect to Y^{3+}, with the initial Tb^{3+} concentration in the solution being 10 at%.

A rocking curve measurement was performed for the (0 4 0) reflection of a pure KYW layer on a KYW substrate. The layer thickness was 14 μm. Therefore, we assumed that the contribution of the substrate peak was negligible. The derived FWHM was only 0.098°, which confirmed a high structural quality of the layer.

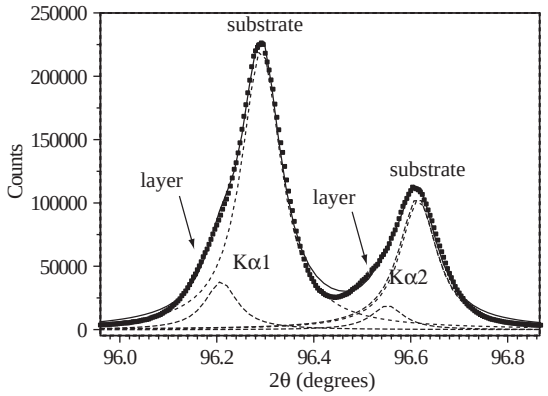

Fig. 4. Detail of the (0 10 0) Bragg reflection of a 10 at% Tb-doped KYW layer on a KYW substrate. Superposed reflections of the $CuK_{\alpha 1}$ and $CuK_{\alpha 2}$ radiation for layer and substrate were fitted with four Lorentzian functions.

3.3. Layer composition and incorporation of Tb^{3+}, Dy^{3+}, or Yb^{3+}

The compositions of the layers were investigated by elemental X-ray fluorescence spectrometry (XRF) using a Kevex–Omicron system. An excitation energy of 40 keV allowed simultaneous quantitative determination of all cations (K and Y on K-lines, W on L-lines). The atomic concentrations of the cations in a 14-μm thick KYW layer, measured against a KYW single-crystal standard grown by the TSSG method, are given in Table 2 together with the theoretical cation concentrations of the stoichiometric KYW compound. Within the experimental statistical error, the compositions of layer and single crystal are the same, as is expected from homoepitaxial growth. However, when measuring the layer against a standard of pressed powders of K_2WO_4 and Y_2O_3, we observed a slight deviation (Table 2). This deviation may not be attributed to a non-stoichiometry of layer and single crystal but may arise from the difference in structure and aggregation state between the powder standard and the investigated samples, i.e., from a systematic error of the XRF method. In the literature, a 5% error is generally accepted for phase identification. In order to determine the exact composition of KYW, a different, independent cross-check analysis would be necessary. Off-stoichiometric values of $KY(WO_4)_2$ were reported previously [23], however, those investigations also lacked an independent cross-check.

The doping levels of RE ions were investigated by electron probe microanalysis (EPMA) using a Cameca SX50 model with an acceleration voltage of 20 kV. The average distribution coefficient, *k*, for Tb^{3+} and Dy^{3+} ions is close to unity, whereas the incorporation of Yb^{3+} appears to be lower due to the highest negative misfit of its ionic radius

Table 2
The stoichiometric and experimental cation composition of a 14-μm thick undoped KYW layer measured by XRF

Compound	Standard	K (at%)	Y (at%)	W (at%)
KYW	Stoichiometric formula	25.0	25.0	50.0
KYW layer	KYW single crystal	24.8±0.3	25.0±0.3	50.2±0.5
KYW layer	K_2WO_4 and Y_2O_3 powders	23.1±0.3	25.0±0.3	51.9±0.5

The indicated errors are statistical experimental errors and do not include systematic errors of the XRF method

Table 3
Incorporation of RE ions into KYW thin layers measured by EPMA

RE ion	Initial conc. in solution (at%)	Actual conc. in layer (at%)	Distribution coefficient k	Ionic radius (Å) [22]
Tb^{3+}	0.50	0.51		
	2.00	2.12	1.04 ± 0.03	1.040
Dy^{3+}	2.00	2.18		
	5.00	4.08	1.00 ± 0.16	1.027
	10.00	11.05		
Y^{3+}				1.019
Yb^{3+}	1.00	1.07		
	5.00	2.67	0.82 ± 0.27	0.985
	10.00	8.43		

k-errors are standard deviations.

with that of the substituted Y^{3+} ion (Table 3). Ions with an ionic radius slightly larger than that of the substituted ion may incorporate better into oxide crystals than those with smaller ionic radius [24]. The mean values of the distribution coefficient in Table 3 support this tendency. However, the standard deviations of our few measurements are too large to confirm unambiguously that RE-ion incorporation decreases in the series $Tb^{3+} > Dy^{3+} > Yb^{3+}$. Comparable differences in the distribution coefficient of the same ion in the same host were also observed during the TSSG growth of KGdW bulk crystals doped with Pr^{3+}, Nd^{3+}, or Er^{3+} [9,25–27].

Other impurity ions could not be detected in our grown KYW layers by XRF or EPMA.

3.4. Waveguiding in RE-doped KYW thin layers

The incorporation of RE ions increases the refractive index of a layer as compared to the undoped substrate. Therefore, the best grown crack-free layer was tested as a planar waveguide. Both end-faces of the sample as well as the layer surface were polished and laser light was coupled into the 2.5-μm thick, 10 at % Tb^{3+}-doped KYW layer along the crystallographic a-direction by focusing with a $25\times$ microscope objective. The out-coupled light was imaged onto the sensor of a CCD-camera using a $10\times$ microscope objective. Passive planar waveguiding of 633-nm light from a helium–neon laser was observed. In addition, active waveguiding was demonstrated by coupling argon-ion laser light at 488 nm into the waveguide to excite the Tb^{3+} ions, which exhibited fluorescence waveguiding in the yellow and red spectral regions. A filter was used to block the residual pump radiation transmitted through the waveguide. The guided fluorescence outcoupled from the sample is shown in Fig. 5.

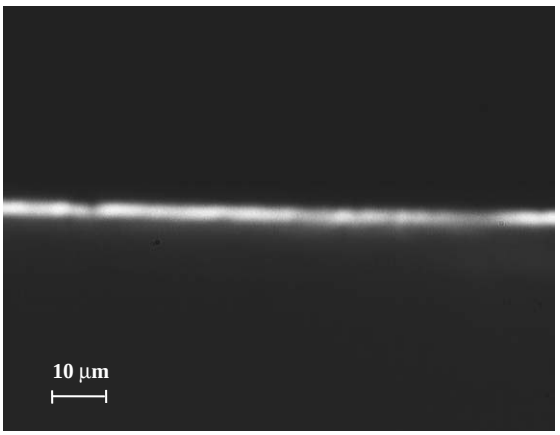

Fig. 5. Image of the guided fluorescence outcoupled from a KYW:10 at % Tb^{3+} planar waveguide.

4. Conclusions

Crystalline layers of RE-ion doped α−KYW have been grown onto single-crystal KYW substrates using LPE from a low-temperature flux at growth temperatures as low as 550–530°C, which can be important for reducing thermal stresses in the grown layers. The growth started by island formation, which then coalesced into a uniform

epitaxial layer of up to 0.5 cm^2. The layers were typically 5–10 μm thick and strictly oriented in the [0 1 0] direction. Although the precipitation of parasitic $nY_2O_3 \times mWO_3$ phases on the bottom of the crucible was observed, the grown layers contained only the KYW phase. The estimated values of the distribution coefficients of RE ions show a tendency toward decreasing incorporation in the series $Tb^{3+} > Dy^{3+} > Yb^{3+}$. The high optical quality of the RE-ion doped KYW layers was confirmed by the demonstration of passive and active planar waveguiding. Taking into account the great potential of RE-ion doped KYW as a laser material, these layers are promising for the implementation as active waveguide devices and may be structured by, e.g., reactive ion etching [28] to channel waveguide lasers and amplifiers.

Acknowledgements

The authors thank Kurt J. Schenk and Daniel Ariosa for their help with the XRD measurements, Alain Volentik for the EPMA measurements, and Raymond Houriet for the XRF measurements. Ana Aznar and members of her research group from the Universitat Rovira i Virgili, Tarragona, Spain, are thanked for their contribution to our initial layer-growth experiments and for helpful discussions. Nikolai Kuleshov is thanked for providing undoped KYW crystals used as substrates. This work was partially supported by the Swiss National Science Foundation.

References

[1] J.M. Esmeria, H. Ishii, M. Sato, H. Ito, Opt. Lett. 20 (1995) 1538.
[2] X. Han, L. Zhang, M. Qiu, G. Wang, Mater Res. Innovat. 7 (2003) 355.
[3] I.V. Mochalov, Opt. Eng. 36 (1997) 1660.
[4] P. Klopp, U. Griebner, V. Petrov, X. Mateos, M.A. Bursukova, M.C. Pujol, R. Solé, J. Gavaldà, M. Aguilò, F. Güell, J. Massons, T. Kirilov, F. Diaz, Appl. Phys. B 74 (2002) 185.
[5] A.A. Kaminskii, J.B. Gruber, S.N. Bagaev, K. Ueda, U. Hömmerich, J.T. Seo, D. Temple, B. Zandi, A.A. Kornienko, E.B. Dunina, A.A. Pavlyuk, R.F. Klevtsova, F.A. Kuznetsov, Phys. Rev. B 65 (2002) 125108.
[6] G. Wang, Z. Luo, J. Crystal Growth 102 (1990) 765.
[7] G. Métrat, N. Muhlstein, A. Brenier, G. Boulon, Opt. Mater. 8 (1997) 75.
[8] A.A. Demidovich, A.N. Kuzmin, G.I. Ryabtsev, M.B. Danailov, W. Strek, A.N. Titov, J. Alloys Compounds. 300–301 (2000) 238.
[9] R. Solé, V. Nikolov, X. Ruiz, J. Gavaldà, X. Solans, M. Aguilò, F. Diaz, J. Crystal Growth 169 (1996) 600.
[10] P.A. Atanasov, R.I. Tomov, J. Perriére, R.W. Eason, N. Vainos, A. Klini, A. Zherikhin, E. Millon, Appl. Phys. Lett. 76 (2000) 2490.
[11] B. Ferrand, B. Chambaz, M. Couchaud, Opt. Mater. 11 (1999) 101.
[12] I. Il'yasov, A.G. Bergman, Zh. Neorg. Khim. 7 (1962) 695.
[13] T.C. Brunold, H.U. Güdel, Chem. Phys. Lett. 249 (1996) 77.
[14] D. Ehrentraut, M. Pollnau, J. Crystal Growth 234 (2002) 533.
[15] D. Ehrentraut, M. Pollnau, S. Kück, Appl. Phys. B 75 (2002) 59.
[16] Y.E. Romanyuk, D. Ehrentraut, M. Pollnau, S. García-Revilla, R. Valiente, Appl. Phys. A 79 (2004) 613.
[17] S. Zuca, R. Borgan, Rev. Chimie 19 (1974) 553.
[18] T. Kawaguchi, D.H. Yoon, M. Minakata, Y. Okada, M. Imaeda, T. Fukuda, J. Crystal Growth 152 (1995) 87.
[19] T. Hanh (Ed.), International Tables for Crystallography, Vol. A, Reidel, Dordrecht, 1992.
[20] K.-H. Hellwege, A.M. Hellwege (Eds.), Numerical Data and Functional Relationships in Science and Technology, Landolt-Börnstein series, Part f, Vol. III/7, Springer, Berlin, 1977.
[21] E. Bauer, Z. Kristallogr. 110 (1958) 395.
[22] R.D. Shannon, Acta Crystallogr A 32 (1976) 751.
[23] E. Gallucci, C. Goutaudier, G. Boulon, M.Th. Cohen-Adad, B.F. Mentzen, J. Crystal Growth 209 (2000) 895.
[24] K. Nassau, The Chemistry of Laser Crystals, in: R. Wolfe (Ed.), Applied Solid State Science: Advances in Materials and Device Research, Vol. 2, Academic Press, New York, 1971, pp. 188–189.
[25] M.C. Pujol, R. Solé, V. Nikolov, Jna. Gavaldà, J. Massons, C. Zaldo, M. Aguiló, F. Diaz, J. Mater. Res. 14 (1999) 3739.
[26] M.C. Pujol, M. Rico, C. Zaldo, R. Solé, V. Nikolov, X. Solans, M. Aguilo, F. Diaz, Appl. Phys. B 68 (1999) 187.
[27] N. Manuilov, V. Nikolov, G. Gentscheva, P. Peshev, J. Crystal Growth 196 (1999) 181.
[28] A. Crunteanu, M. Pollnau, G. Jänchen, C. Hibert, P. Hoffmann, R.P. Salathé, R.W. Eason, C. Grivas, D.P. Shepherd, Appl. Phys. B 75 (2002) 15.